CESifo WORKING PAPERS

10556
2023

July 2023

Trends and Persistence in the Greenland Ice Sheet Mass

Guglielmo Maria Caporale, Luis Alberiko Gil-Alana, Laura Sauci

CESifo

Impressum:

CESifo Working Papers
ISSN 2364-1428 (electronic version)
Publisher and distributor: Munich Society for the Promotion of Economic Research - CESifo GmbH
The international platform of Ludwigs-Maximilians University's Center for Economic Studies and the ifo Institute
Poschingerstr. 5, 81679 Munich, Germany
Telephone +49 (0)89 2180-2740, Telefax +49 (0)89 2180-17845, email office@cesifo.de
Editor: Clemens Fuest
https://www.cesifo.org/en/wp
An electronic version of the paper may be downloaded
· from the SSRN website: www.SSRN.com
· from the RePEc website: www.RePEc.org
· from the CESifo website: https://www.cesifo.org/en/wp

CESifo *Working Paper No. 10556*

Trends and Persistence in the Greenland Ice Sheet Mass

Abstract

This paper examines trends and persistence in the Greenland ice sheet mass by applying fractional integration methods to a dataset constructed by Mankoff et al. (2020) on ice discharge for seven different regions of Greenland. The adopted empirical framework encompasses a wide range of stochastic processes and is informative about their dynamic and long-run properties. The main finding is that significant changes have occurred in the behaviour of the series of interest in recent years; more specifically, although a deterministic trend is not present, ice discharge in the various regions of Greenland has become a non-stationary, explosive process, with shocks having permanent effects. It appears that, as a result of global warming, the ice mass loss in Greenland has already reached a tipping point and become an irreversible process.

JEL-Codes: C220, Q540.

Keywords: Greenland ice sheet mass, long memory, fractional integration, persistence, trends.

Guglielmo Maria Caporale
Department of Economics and Finance
Brunel University London
United Kingdom – Uxbridge, UB8 3PH
Guglielmo-Maria.Caporale@brunel.ac.uk

Luis Alberiko Gil-Alana
University of Navarra
Pamplona / Spain
alana@unav.es

Laura Sauci
Universidad de la Rioja
Logroño / Spain

July 2023
Luis A. Gil-Alana gratefully acknowledges financial support from the MINEIC-AEI-FEDER PID2020-113691RB-I00 project from 'Ministerio de Economía, Industria y Competitividad' (MINEIC), 'Agencia Estatal de Investigación' (AEI) Spain and 'Fondo Europeo de Desarrollo Regional' (FEDER), and also from Internal Projects of the Universidad Francisco de Vitoria.

1. Introduction

The Greenland ice sheet is a vast body of ice covering approximately 80% of the surface of Greenland, and it is the second largest ice body in the world after the Antarctic ice sheet. Global warming has been affecting it severely because of the so-called polar amplification, i.e. the fact that changes in temperature resulting from greenhouse effects are larger than the average in geographical areas near the poles as in the case of Greenland. Specifically, the Greenland ice sheet has been melting and it is feared that if this process continues it will gradually reach a tipping point making it irreversible. For instance, Mouginot et al. (2019) calculated that there had been a sixfold increase in mass loss since the 1980s. Enderlin et al. (2014) provided evidence that surface melting rather than ice discharge was leading to sea level rises. Various other studies such as those by van der Broeke et al. (2017) and by the IMBIE Team (2020) similarly concluded that reduced surface mass balance was the main driver of the ice loss. Choi et al. (2021) argued instead that ice discharge from marine-terminating glaciers would gradually become the main factor driving the total mass loss.

Khan et al. (2015) also reported an increase in ice loss rate caused by speeding up of glaciers and enhanced melting and contributing to a rise in global sea level. In their analysis they used satellite altimetry, airborne altimetry, interferometry, aerial photographs, gravimetry data sets etc.; interestingly, they noticed the presence of short-term fluctuations that could produce erroneous long-term trends if wrongly extrapolated. This implies that using an appropriate modelling framework which enables the researcher to identify correctly the long-run properties of the ice sheet mass data is a crucial issue. The purpose of the present study is to address it by using a long-memory approach that is ideally suited to detecting the presence of long-run trends and measuring the degree of persistence in the series of interest. More specifically, it applies fractional integration

methods which are more general and flexible than standard time series approaches since they allow the differencing parameter d to take any real value, including fractional ones; as a result, this type of models can encompass a wide range of stochastic processes and provide information about whether or not the series is mean-reverting (and thus whether shocks have transitory or permanent effects), the speed of adjustment towards the long-run equilibrium, and various other important dynamic properties of the series under examination. Given the recent evidence on the increasing importance of ice discharge for ice mass loss (see Choi et al., 2021), we focus on this specific factor using the dataset constructed by Mankoff et al. (2020) for seven different regions of Greenland. The results will shed light at the regional level on whether the recently observed ice mass loss is likely to worsen further and will have important implications in terms of the policy actions required to tackle the consequences of climate change for global sea level.

The layout of the paper is the following: Section 2 outlines the econometric modelling framework; Section 3 describes the data and presents the empirical results; Section 4 offers some concluding remarks.

2. Empirical Framework

We assume that the time series under examination follows a long memory process. This is a feature that was first noticed by the hydrologist Hurst (1951) in his analysis of the water level in the Nile river. More specifically, he observed a cyclical persistent pattern in the data that was consistent with a pole or singularity in the spectral density function (Hurst, 1956). More than a decade later this feature was modelled by Mandelbrot (1969) and Mandelbrot and Wallis (1971) using a fractional Gaussian noise (fGn) specification, and subsequently by Granger (1980), Granger and Joyeux (1980) and Hosking (1981) by means of the AutoRegressive Fractionally Integrated Moving Average (ARFIMA) model.

Nowadays, it is widely accepted that long memory is a property of many time series in the fields of hydrology, climatology, environmental studies, and economics and finance.

If one defines the spectral density function of a covariance stationary process as the Fourier transform of its autocovariances, i.e.,

$$f(\lambda)\ ) = \sum_{j=-\infty}^{\infty} \gamma(u) e^{j\lambda u} = \sum_{j=-\infty}^{\infty} \gamma(u) \cos(\lambda u). \qquad (1)$$

where $\gamma(u) = E[(x(t) - \mu)\ (x(t+u) - \mu)]$ and μ is the mean of the stationary process x(t), one can then say that this process displays the property of long memory (LM) or long-range dependence (LRD) if its spectral density contains at least one pole or singularity in the interval $[0, \pi)$, i.e.,

$$f(\lambda) \rightarrow \infty, \quad \text{for some } \lambda \in [0, \pi). \qquad (2)$$

The corresponding definition in the time domain is that the infinite sum of the autocovariances is infinite, i.e.,

$$\sum_{j=-\infty}^{\infty} |\gamma(u)| = \infty. \qquad (3)$$

Among the many models that satisfy these statistical properties, a very simple and useful one is based on the fractional differencing parameter d, within the class of fractional integration or I(d) models described by:

$$(1 - L)^d\ x(t) = u(t)\ \ t = 0, \pm 1, ... \qquad (3)$$

where L is the lag operator, i.e., $L^k x(t) = x(t-k)$, and u(t) is by definition an integrated of order 0 or I(0) (also called short memory, SM) process characterised by a positive and bounded spectral density function, i.e.:

$$0 < f(\lambda) < \infty, \qquad (4)$$

or, alternatively, in the time domain, by an infinite sum of the autocovariances which is finite, i.e.:

$$\sum_{j=-\infty}^{\infty} |\gamma(u)| < \infty. \qquad (5)$$

Within the category of SM processes, the simplest model is the white noise one, which does not allow time dependence. However, stationary ARMA processes also belong to this category. Thus, if u(t) in (3) is an ARMA(p, q) process, x(t) is said to be an AutoRegressive Fractionally Integrated Moving Average, ARFIMA(p, d, q) process, where d is the number of differences required to make x(t) an ARMA(p, q) process.

Allowing d to be a fractional value opens a wide range of possibilities; specifically, if d = 0, x(t) = u(t) and the process exhibits short memory; if d belongs to the interval (0, 0.5), x(t) displays the property of long memory since the spectral density function is unbounded at the zero frequency, i.e.,

$$f(\lambda) \rightarrow \infty \quad \text{as} \quad \lambda \rightarrow 0^{+}. \qquad (6)$$

Long memory refers to the high degree of association between observations which are far apart in time, where the process in (3) can be rewritten, for any real d, as:

$$x(t) = \mathrm{d}\, x(t-1) - \frac{\mathrm{d}(\mathrm{d}-1)}{2} x(t-2) + \frac{\mathrm{d}(\mathrm{d}-1)(\mathrm{d}-2)}{6} x(t-3) - \ldots + u(t),$$

Further, if $0.5 \leq \mathrm{d} < 1$, the process is non-stationary though mean-reverting, shocks having only temporary effects, while values of $\mathrm{d} \geq 1$ imply that they have permanent effects.

In the empirical application presented below we consider the following model:

$$y_t = \beta_0 + \beta_1 t + x_t, \qquad (1-L)^d x_t = u_t, \qquad u_t = \phi u_{t-12} + \varepsilon_t, \qquad (7)$$

where y_t indicates the series of interest, and β_0 and β_1 stand respectively for the intercept and the coefficient on a linear time trend; in addition, the error term x_t is assumed to be integrated of order d, where L is the lag operator, i.e., $L^k x_t = x_{t-k}$, and u_t is I(0) and is modelled as a seasonal AR(1) process as specified in (7) given the monthly frequency of the data. The estimation is carried out using the Whittle function in the frequency domain.

3. Data and Empirical Results

For the empirical analysis we use the monthly data from Mankoff et al. (2020) for the period 1986:04 - 2022:10 on the Greenland Ice Sheet solid ice discharge, more precisely on 'all discharging ice that flows faster than 100 m yr−1'. Following Mouginot et al. (2019), the data have been collected for seven different regions, namely: central east (CE), central west (CW), northeast (NE), north (NO), northwest (NW), southeast (SE) and southwest (SW) – see Figure 1.

Figure 1. Ice discharge regions in Greenland.

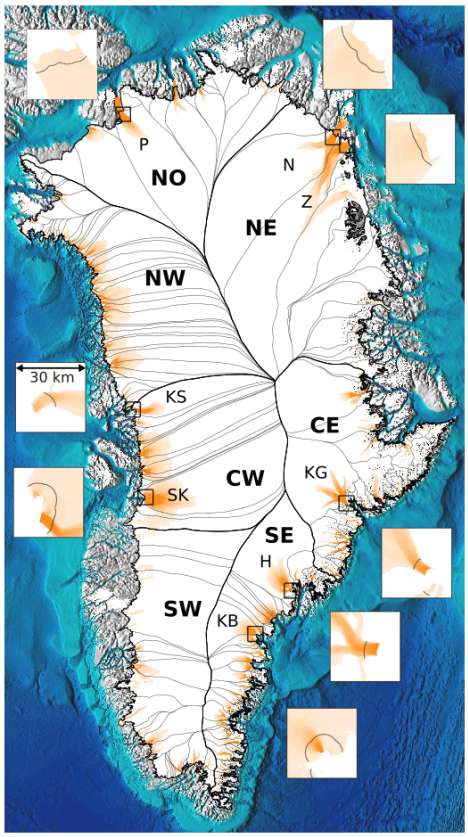

Source: Mankoff et al. (2020), following Mouginot et al. (2019)
(Orange denotes ice discharge that flows faster than 100 m yr−1)

Table 1 displays the estimates of the differencing parameter d for three different model specifications, i.e. (i) without deterministic terms (column 2), (ii) with an intercept only (column 3), and (iii) with an intercept and a linear time trend (column 4), where the

coefficients in bold are those from the models selected on the basis of the statistical significance of the regressors, namely one with an intercept as well as a time trend in the case of NE, and one with an intercept only in the remaining cases.

TABLES 1 AND 2 ABOUT HERE

Table 2 reports the estimates of d as well as of the other coefficients. It can be seen that the estimated values of d are relatively high in all cases, ranging from 0.72 (NO) and 0.79 (SE) to 1.13 (SW). Evidence of mean reversion (i.e., estimates of d that are significantly smaller than 1) is found in the case of NO (0.72), SE (0.79), CE and NE (0.82), and NW (0.84). By contrast, the unit root null hypothesis (d = 1) cannot be rejected in the case of CW (d = 0.93) and SW (d = 1.13). Finally, the seasonal AR coefficient is relatively low in all cases.

Next, the possibility of structural breaks is taken into account. For this purpose we use a procedure developed in Gil-Alana (2008) which is essentially an extension of the Bai and Perron's (2003) tests to the fractional case. We only allow for a single break in order to ensure that the subsamples are sufficiently large. Table 3 reports the break dates, which are surprisingly different for each of the series: 2000 for CW, 2002 for CE, 2003 for SE, 2007 for SW, 2010 for NW, 2013 for NE, and 2014 for NO.

TABLES 3 AND 4 ABOUT HERE

Table 4 displays the sub-sample estimates of d. It can be seen that in the case of the first ones almost all the estimated values are smaller than 1, which implies mean-reverting behaviour and only transitory effects of shocks. The single exception is the estimate of d in the case of SW, which is smaller than 1 (0.96), though the confidence interval includes the value of 1. By contrast, in the second sub-samples mean reversion does not occur in any case. The unit root null cannot be rejected for CE, NW and SE,

whilst this hypothesis is rejected in favour of values of d above 1 in all the remaining cases. Note also that the time trend is insignificant in all cases in both sub-samples.

To sum up, despite some regional variations, the general picture suggests that, although no deterministic trend is present, changes have occurred in recent years that have made the ice discharge an explosive process, with shocks such as global warming having permanent effects, which is a very concerning finding for the global sea level and the planet Earth as a whole.

5. Conclusions

This paper has examined trends and persistence in the Greenland ice sheet mass by using a dataset constructed by Mankoff et al. (2020) on ice discharge for seven different regions of Greenland. This has been identified by previous studies (see Choi et al., 2021) as an increasingly important determinant of the ice mass loss in Greenland, and therefore it is also the focus of the present one.

Our empirical analysis is based on a very general, fractional integration modelling framework that enables us to consider a wide range of stochastic processes and to obtain informative evidence about their dynamic and long-run properties. The main finding of our study is that significant changes have occurred in the behaviour of the series of interest in recent years; more specifically, although a deterministic trend is not present, ice discharge in the various regions of Greenland has become a non-stationary, explosive process, with shocks having irreversible effects.

The external factor that has caused these changes can most plausibly be identified as global warming. Our evidence suggests that its impact has been such that the ice mass loss in Greenland might already have reached a tipping point, and thus that it might be too late to take action to stop it. In fact in the "Climate Change 2023 – Synthesis Report"

the UN Intergovernmental Panel on Climate Change (IPCC) concludes that “global warming will continue to increase in the near term (2021-2040) mainly due to increased cumulative CO_2 emissions in nearly all considered scenarios and modelled pathways. In the near term, global warming is more likely than not to reach 1.5°C even under the very low GHG emission scenario (SSP1-1.9) and likely or very likely to exceed 1.5°C under higher emissions scenarios. In other words, there is no evidence that current policies are succeeding in reducing carbon emissions, and therefore the expectation is that global warming will keep worsening. As a result, the most likely scenario is that the ice mass loss in Greenland will be reduced even further over time, as implied by our empirical results.

References

Bai, J. and P. Perron (2003), Bai, J., & Perron, P. (2003), Computation and analysis of multiple structural change models. Journal of Applied Econometrics, 18, 1-22.

Choi, Y., Morlighem, M., Rignot, E. and M. Wood (2021), Ice dynamics will remain a primary driver of Greenland ice sheet mass loss over the next century, Communications Earth & Environment, 2, article number 26.

Enderlin, E.M., Howat, I.M., Jeong, S., Noh, M.-J., van Angelen, J.H. and M. R. van den Broeke (2014), An improved mass budget for the Greenland ice sheet, Geophysical Research Letters, https://doi.org/10.1002/2013GL059010

Gil-Alana, L.A. (2008), Fractional integration and structural breaks at unknown periods of time, Journal of Time Series Analysis 29, 1, 163-185.

Granger, C.W.J. (1980), Long memory relationships and the aggregation of dynamic models, Journal of Econometrics 14, 2, 227-238.

Granger, C.W.J. and R. Joyeux (1980), An Introduction to Long Memory Time Series Models and Fractional Differencing, Journal of Time Series Analysis 1, 1, 15-29.

Hosking, J.R.M. (1981) Fractional differencing.Biometrika, 68, 168–176.

Hurst, H.E. (1956), The Problem of Long-Term Storage in Reservoirs, Hydrology Science Journal 1, 13–27.

IMBIE Team (2020), Mass balance of the Greenland Ice Sheet from 1992 to 2018, Nature, 579, 233–239.

IPCC (Intergovernmental Panel on Climate Change) (2023), "Climate Change 2023 – Synthesis Report", United Nations, https://www.ipcc.ch/report/ar6/syr/

Khan, S.A., Aschwanden, A., Bjørk, A.A., Wahr, J.,Kjeldsen, K.K. and K.H. Kjær (2015), Greenland ice sheet mass balance: a review, Reports on Progress in Physics, 78, 046801

Mandelbrot, B., (1971), A Fast Fractional Gaussian Noise Generator, Water Resources Research 7, 3, 543-553.

Mandelbrot, B. and J.R. Wallis (1971), Computer Experiments With Fractional Gaussian Noises: Part 1, Averages and Variances, Water Resources Research 5, 1, 228-241.

Mankoff, K.D., Solgaard, A., Colgan, W., Ahlstrøm, A.P., Khan, S.A., and Fausto, R.S. (2020). Greenland Ice Sheet solid ice discharge from 1986 through March 2020, Earth System Science Data, 12, 1367–1383.

Mouginot, J., Rignot, E., Bjørk, A.A. and M. Wood (2019), Forty-six years of Greenland Ice Sheet mass balance from 1972 to 2018, Earth, Atmospheric, and Planetary Sciences, https://doi.org/10.1073/pnas.1904242116

van den Broeke, M., Box, J., Fettweis, X., Hanna, E., Noël, B., Marco Tedesco, Dirk van As, Willem Jan van de Berg & Leo van Kampenhout (2017), Greenland Ice Sheet Surface Mass Loss: Recent Developments in Observation and Modeling, Climate Change Reports, 3, 345–356.

Table 1: Estimates of the integration order, d

Series	No deterministic terms	An intercept	An intercept and a linear time trend
CE	0.98 (0.92, 1.06)	**0.82 (0.74, 0.93)**	0.82 (0.74, 0.93)
CW	1.02 (0.96, 1.11)	**0.93 (0.85, 1.02)**	0.93 (0.85, 1.02)
NE	0.97 (0.90, 1.04)	0.82 (0.75, 0.90)	**0.82 (0.74, 0.90)**
NO	0.97 (0.91, 1.05)	**0.72 (0.64, 0.82)**	0.72 (0.64, 0.83)
NW	1.00 (0.94, 1.07)	**0.84 (0.77, 0.93)**	0.84 (0.78, 0.93)
SE	0.99 (0.93, 1.06)	**0.79 (0.74, 0.85)**	0.79 (0.74, 0.85)
SW	1.01 (0.95, 1.10)	**1.13 (1.04, 1.24)**	1.13 (1.04, 1.24)

In parenthesis the 95% confidence bands for the estimates of d. Values in bold are from the selected specification on the basis of the statistical significance of the regressors for each series.

Table 2: Estimated coefficients for the selected models

Series	No deterministic terms	An intercept	An intercept and a linear time trend	Seasonality
CE	0.82 (0.74, 0.93)	67.4768 (44.68)	-----	0.083
CW	0.93 (0.85, 1.02)	69.9414 (45.30)	-----	0.039
NE	0.82 (0.74, 0.90)	22.6266 (50.49)	0.0170 (2.37)	0.029
NO	0.72 (0.64, 0.82)	22.6801 (32.98)	-----	0.019
NW	0.84 (0.77, 0.93)	93.7503 (63.43)	-----	-0.050
SE	0.79 (0.74, 0.85)	144.2837 (79.95)	-----	-0.013
SW	1.13 (1.04, 1.24)	20.5382 (59.82)	-----	-0.028

The values in parenthesis in columns 2 and 3 are the corresponding t-statistics for each series.

Table 3: Break dates detected using the Bai and Perron (2003) tests

Series	Break date
CE	October 2002
CW	February 2000
NE	October 2013
NO	March 2014
NW	October 2010
SE	February 2003
SW	June 2007

A single break is allowed for each series.

Table 4: Estimated coefficients before and after the breaks

Series	No deterministic terms	An intercept	An intercept and a linear time trend	Seasonality
i) First sub-samples				
CE	0.73 (0.56, 0.99)	67.8587 (28.33)	---	0.143
CW	0.57 (0.43, 0.81)	71.2801 (40.92)	---	0.078
NE	0.76 (0.67, 0.88)	22.7247 (37.64)	---	0.044
NO	0.59 (0.46, 0.76)	23.2706 (29.62)	---	0.011
NW	0.81 (0.71, 0.94)	93.8201 (55-66)	---	-0.067
SE	0.66 (0.57, 0.77)	143.1049 (58.05)	---	-0.027
SW	0.96 (0.83, 1.14)	20.5364 (45.84)	---	-0.004
i) Second sub-samples				
CE	0.93 (0.85, 1.03)	74.4772 (82.36)	---	-0.113
CW	1.11 (1.01, 1.22)	77.7730 (67.08)	---	0.017
NE	1.17 (1.06, 1.31)	26.5309 (37.64)	---	-0.083
NO	1.31 (1.18, 1.47)	24.9734 (29.62)	---	-0.0006
NW	0.87 (0.77, 1.00)	103.8391 (55.66)	---	-0.034
SE	0.91 (0.84, 1.00)	137.1984 (58.05)	---	-0.010
SW	1.22 (1.11, 1.35)	19.7333 (45.84)	---	-0.074

The time trend coefficient is insignificant in all cases.